



**University of
Zurich**^{UZH}

**Zurich Open Repository and
Archive**

University of Zurich
University Library
Strickhofstrasse 39
CH-8057 Zurich
www.zora.uzh.ch

Year: 2016

Fluorescent Base Analogue Reveals T-HgII-T Base Pairs Have High Kinetic Stabilities That Perturb DNA Metabolism

Schmidt, Olivia P ; Mata, Guillaume ; Luedtke, Nathan W

Abstract: The thymidine analogue DMAT was used for the first fluorescence-based study of direct, site-specific metal binding reactions involving unmodified nucleobases in duplex DNA. The fluorescence properties of DMAT-A base pairs were highly sensitive to mercury binding reactions at T-T mismatches located at an adjacent site or one base pair away. This allowed for precise determination of the local kinetic and thermodynamic parameters of T-HgII-T binding reactions. The on- and off-rates of HgII were surprisingly slow, with association rate constants (k_{on}) 10^4 – 10^5 M⁻¹ s⁻¹, and dissociation rate constants (k_{off}) 10^{-4} – 10^{-3} s⁻¹; giving equilibrium dissociation constants (K_d) = 8–50 nM. In contrast, duplexes lacking a T-T mismatch exhibited local, nonspecific HgII binding affinities in the range of K_d = 0.2–2.0 M, depending on the buffer conditions. The exceptionally high kinetic stabilities of T-HgII-T metallo-base pairs (half-lives = 0.3–1.3 h) perturbed dynamic processes including DNA strand displacement and primer extension by DNA polymerases that resulted in premature chain termination of DNA synthesis. In addition to providing the first detailed kinetic and thermodynamic parameters of site-specific T-HgII-T binding reactions in duplex DNA, these results demonstrate that T-HgII-T base pairs have a high potential to disrupt DNA metabolism *in vivo*.

DOI: <https://doi.org/10.1021/jacs.6b09044>

Posted at the Zurich Open Repository and Archive, University of Zurich

ZORA URL: <https://doi.org/10.5167/uzh-134705>

Journal Article

Accepted Version

Originally published at:

Schmidt, Olivia P; Mata, Guillaume; Luedtke, Nathan W (2016). Fluorescent Base Analogue Reveals T-HgII-T Base Pairs Have High Kinetic Stabilities That Perturb DNA Metabolism. *Journal of the American Chemical Society*, 138(44):14733-14739.

DOI: <https://doi.org/10.1021/jacs.6b09044>

Fluorescent Base Analog Reveals T-Hg^{II}-T Base Pairs Have High Kinetic Stabilities that Perturb DNA Metabolism

Olivia P. Schmidt, Guillaume Mata and Nathan W. Luedtke*

Department of Chemistry, University of Zürich, Winterthurerstrasse 190, CH-8057 Zürich, Switzerland

ABSTRACT: The thymidine analog ^{DMA}T was used for the first fluorescence-based study of direct, site-specific metal binding reactions involving unmodified nucleobases in duplex DNA. The fluorescence properties of ^{DMA}T-A base pairs were highly sensitive to mercury binding reactions at T-T mismatches located at an adjacent site or one base pair away. This allowed for precise determination of the local kinetic and thermodynamic parameters of T-Hg^{II}-T binding reactions. The on- and off-rates of Hg^{II} were surprisingly slow, with association rate constants (k_{on}) $\approx 10^4 - 10^5 \text{ M}^{-1} \text{ s}^{-1}$, and dissociation rate constants (k_{off}) $\approx 10^{-4} - 10^{-3} \text{ s}^{-1}$, giving equilibrium dissociation constants (K_d) = 8 – 50 nM. In contrast, duplexes lacking a T-T mismatch exhibited local, non-specific Hg^{II} binding affinities in the range of K_d = 0.2 – 2.0 μM , depending on the buffer conditions. The exceptionally high kinetic stabilities of T-Hg^{II}-T metallo-base pairs (half-lives = 0.3 – 1.3 h) perturbed dynamic processes including DNA strand-displacement and primer extension by DNA polymerases that resulted in premature chain termination of DNA synthesis. In addition to providing the first detailed kinetic and thermodynamic parameters of site-specific T-Hg^{II}-T binding reactions in duplex DNA, these results demonstrate that T-Hg^{II}-T base pairs have a high potential to disrupt DNA metabolism *in vivo*.

INTRODUCTION

Hg^{II} is infamous for being cytotoxic and mutagenic,¹ but the exact mechanisms for these activities are still unclear. In addition to oxidative stress,² Hg^{II} causes DNA point mutations,³ DNA strand breaks,^{4,5} and the inhibition of DNA synthesis and repair in live cells.^{5,6} These activities could be the result of direct mercury-DNA binding interactions. When 5 μM of HgCl₂ was applied to live cells for 4 h and the DNA harvested and analyzed, approximately 0.3 % of base pairs contained mercury.⁷ After 30 years of study, however, little is known about the composition or structure of these complexes. While many different metal-DNA binding modes are possible,⁸ Hg^{II} preferentially binds to N1 or N7 of purines and to N3 of thymidine residues *in vitro*.⁹ In 2006, Ono and co-workers reported that T-T mismatches in duplex DNA exhibited stoichiometric binding of Hg^{II} ions *in vitro*, giving duplexes with approximately the same thermal stabilities as duplexes containing T-A base pairs.¹⁰ The preferred Hg^{II} binding site was found to be the N3 positions of two deprotonated thymine residues (Figure 1a).¹¹ A crystal structure of duplex DNA containing two such T-Hg^{II}-T base pairs revealed minimal distortion of the B-form duplex.¹² In addition to structural similarities, T-Hg^{II}-T can serve as a functional mimic of T-A base pairs by stabilizing T-T during DNA primer extension,¹³ and by causing the enzymatic misincorporation of dTTP across from thymidine to give T-Hg^{II}-T base pairs.¹⁴ These activities provide a potential mechanism for the formation of T-Hg^{II}-T base pairs in S-phase cells.

Given the potentially broad importance of T-Hg^{II}-T base pairs in both biological and material sciences,¹⁵ a wide variety of spectroscopic methods have been used to characterize their properties including UV,^{10,16} Raman,¹⁷ CD,¹⁸ NMR,¹⁹ ITC,²⁰ and fluorescence.²¹ With the exception of high resolution structural analyses by Raman and NMR, these methods report changes in global properties resulting from both specific and non-specific binding interactions. To our knowledge, there are no previous studies that report the exact kinetic and thermodynamic parameters of local, site-specific T-Hg^{II}-T binding reactions in duplex DNA. These values are important for understanding the potential biological impact and material properties of T-Hg^{II}-T base pairs.

Fluorescent nucleobase analogs (FBAs) can facilitate highly sensitive biophysical measurements with single-base resolution.^{22,23} FBAs are therefore ideal candidates for characterizing local binding interactions,²⁴ but only a few previous studies have utilized FBAs as probes of transition metal binding.²⁵ In these cases, the FBA directly participated in the binding reaction and therefore it provided little or no information about native DNA-metal interactions. In other examples,²⁴ ligand binding caused conformational changes that impacted the FBA's microenvironment and therefore its fluorescence properties in an indirect way. There are no previous examples of native, site-specific metal-nucleobase binding interactions being directly reported by an FBA. This would provide a powerful tool for determining the kinetic and thermodynamic parameters of local metal binding reactions. With this goal, we recently synthesized a new fluorescent thymidine mimic “^{DMA}T” that exhibits same base pairing preferences as native

thymine residues.²⁶ Duplexes containing $\text{DMA}^{\text{T}}\text{-A}$ or $\text{DMA}^{\text{T}}\text{-Hg}^{\text{II}}\text{-T}$ base pairs (Figure 1b) exhibited the same global structures, thermal stabilities, and metal binding properties as wild-type duplexes containing T-A or T-Hg^{II}-T, respectively. Here we report the use of $\text{DMA}^{\text{T}}\text{-T}$ and $\text{DMA}^{\text{T}}\text{-A}$ for directly assessing the local kinetic and thermodynamic parameters of T-Hg^{II}-T binding reactions. Surprisingly, T-Hg^{II}-T complexes exhibited slow association and dissociation kinetics and perturbed dynamic processes including DNA strand displacement and enzymatic synthesis. T-Hg^{II}-T complexes therefore have a high potential to disrupt DNA metabolism *in vivo*.

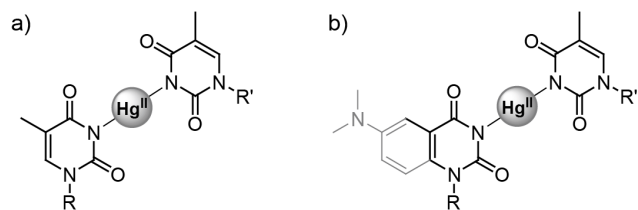


Figure 1. (a) T-Hg^{II}-T base pair. (b) $\text{DMA}^{\text{T}}\text{-Hg}^{\text{II}}\text{-T}$ base pair (R, R' = duplex DNA).

RESULTS

Thermodynamic analysis of T-Hg^{II}-T binding. To the best of our knowledge, isothermal titration calorimetry (ITC) was the only technique previously used to assess the thermodynamic parameters of Hg^{II} binding to T-T mismatches in duplex DNA.²⁰ In this approach, Hg^{II} was titrated into concentrated solutions of DNA (40 μM) and the changes in heat flow were measured. The results suggested a modest equilibrium dissociation constant (K_d) = $\sim 2 \mu\text{M}$ for DNA sequences containing a single T-T mismatch.²⁰ Given the exceptionally high sensitivity of fluorescence measurements, we were able to use dilute solutions of DNA (25 nM, Figure 2) for equilibrium titrations (Figure 3). Initial binding experiments were conducted in the same non-coordinating buffer previously reported for ITC-based measurements (10 mM cacodylic acid, 100 mM NaClO₄ (pH = 6.8)).²⁰ Hg^{II} was titrated into solutions of 21-mer duplex DNA containing either a $\text{DMA}^{\text{T}}\text{-T}$ mismatch (red circles, Figure 3a), or a $\text{DMA}^{\text{T}}\text{-A}$ base pair at position X13 (red triangles, Figure 3a). After equilibrating the DNA with variable Hg^{II} concentrations for 1 h at 25 $^{\circ}\text{C}$, the fluorescence intensities of each sample were measured. By fitting the data to a monophasic equation, K_d values were determined (eq. 1 – 4, SI). To our surprise, both duplexes exhibited very high Hg^{II} affinities under these conditions, with a K_d = $43 \pm 6 \text{ nM}$ for the duplex containing the $\text{DMA}^{\text{T}}\text{-T}$ mismatch and a K_d = $210 \pm 40 \text{ nM}$ for the DNA containing a $\text{DMA}^{\text{T}}\text{-A}$ base pair with no T-T mismatch. We reasoned that this small, 5-fold difference between mismatch-specific and non-specific DNA binding affinities would complicate the study of association kinetics under these conditions. To increase the specificity of binding (blue symbols, Figure 3a), the stringency of the reaction was increased by using a phosphate-citrate buffer (200 mM Na₂HPO₄, 100 mM citric acid and 100 mM NaNO₃ (pH = 7.35)) that reversibly coordinates to mercury ions.²⁷ Remarkably, a very similar affinity was measured for the DNA containing a $\text{DMA}^{\text{T}}\text{-T}$ mismatch in both coordinating (K_d = $77 \pm 4 \text{ nM}$) and non-coordinating buffers (K_d = $43 \pm 6 \text{ nM}$). In contrast,

DNA containing $\text{DMA}^{\text{T}}\text{-A}$ and no T-T mismatch exhibited a 10-fold lower affinity (K_d = $1.97 \pm 0.08 \mu\text{M}$) in the coordinating versus non-coordinating buffers. Given the large improvement in binding specificity, we selected the high-stringency buffer for subsequent experiments.

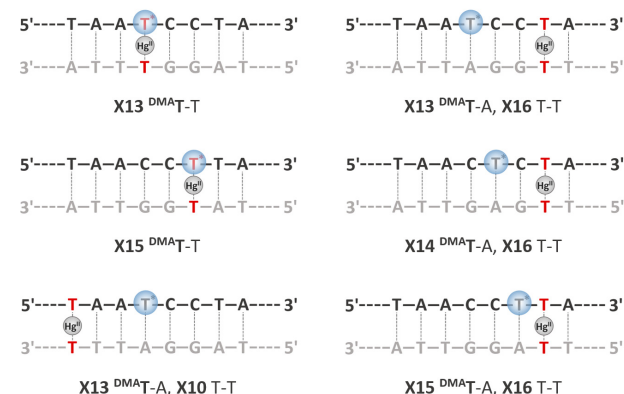


Figure 2. Variable regions (underlined) and names of DNA sequences used in these studies: **X13**: 5'-CCC-TAA-CCC-TAA-XCC-TAA-CCC-3'; **X14**: 5'-CCC-TAA-CCC-TAA-CXC-TAA-CCC-3'; **X15**: 5'-CCC-TAA-CCC-TAA-CCX-TAA-CCC-3'; where **X** = T or T* (DMA^{T}). See Tables S1 – S2 (Supporting Information) for a complete list of all reported duplexes.

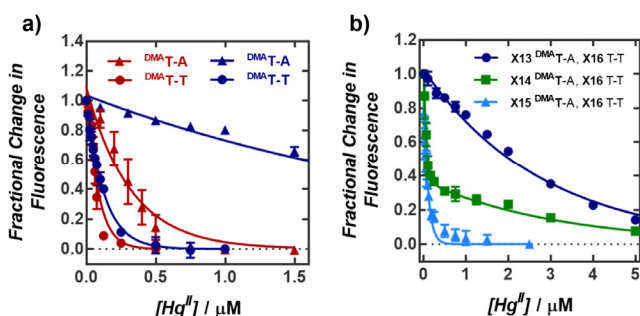


Figure 3. (a) Normalized changes in fluorescence of “X13 $\text{DMA}^{\text{T}}\text{-A}$ ” (triangles) or “X13 $\text{DMA}^{\text{T}}\text{-T}$ ” (circles) upon addition of Hg^{II} in a non-coordinating buffer (red) or metal-coordinating buffer (blue). (b) Fluorescence quenching of three different duplexes containing a T-T mismatch fixed at position X16 and a $\text{DMA}^{\text{T}}\text{-A}$ base pair at position X13, X14, or X15. All DNA samples (25 nM) were incubated with variable concentrations of Hg(ClO₄)₂ at 25 $^{\circ}\text{C}$ for 1 h prior to reading (λ_{ex} = 370 nm, λ_{em} = 500 nm). Samples in a) contained either 10 mM cacodylic acid, 100 mM NaClO₄ (pH = 6.8) or 200 mM of Na₂HPO₄, 100 mM of citric acid, 100 mM NaNO₃ (pH = 7.35). Samples in b) were prepared in the phosphate-citrate buffer. See Figures S2 – S4 for raw data.

To evaluate the ability of a $\text{DMA}^{\text{T}}\text{-A}$ base pair to report the formation of a wild-type T-Hg^{II}-T complex at a neighboring or proximal site, duplexes were prepared containing a T-T mismatch at position X16 and a $\text{DMA}^{\text{T}}\text{-A}$ base pair at position X13, X14, or X15 (Figure 2). The duplex “X13 $\text{DMA}^{\text{T}}\text{-A}$, X16 T-T” containing two intervening base pairs between $\text{DMA}^{\text{T}}\text{-A}$ and T-T exhibited the same concentration-dependent fluorescence response (apparent K_d = $1.96 \pm 0.05 \mu\text{M}$, Figure 3b) as did duplex “X13 $\text{DMA}^{\text{T}}\text{-A}$ ” containing no T-T mismatch (K_d = $1.97 \pm 0.08 \mu\text{M}$, Table 1). This indicated that in the case of “X13 $\text{DMA}^{\text{T}}\text{-A}$, X16 T-T” the probe was positioned too far away ($\sim 10 \text{ \AA}$) from T-T to report site-specific T-Hg^{II}-T asso-

ciation. This is consistent with heavy-atom fluorescence quenching effects that act over very short distances. In contrast, the duplex “X15^{DMA}T-A, X16 T-T” with no intervening base pair between ^{DMA}T-A and T-T exhibited the same apparent affinity ($K_d = 57 \pm 7$ nM) as observed for duplex “X13^{DMA}T-T” ($K_d = 77 \pm 4$ nM, Table 1). These results suggest that the ^{DMA}T-A base pair can report Hg^{II} binding of a neighboring T-T mismatch with little or no impact on the affinity of the reaction. Kinetics analyses (Table 2) further support this conclusion. Interestingly, the duplex “X14^{DMA}T-A, X16 T-T” containing a single intervening base pair between ^{DMA}T-A and T-T exhibited a pronounced bi-phasic quenching curve (green squares, Figure 3b). The first component saturated at a 0.7 fractional decrease in fluorescence with an affinity consistent with specific T-Hg^{II}-T binding ($K_d = 34 \pm 12$ nM), while the second component exhibited an apparent affinity indicative of non-specific binding (apparent $K_d = 2.20 \pm 0.09$ μ M, Table 1, overall goodness of fit (R^2) = 0.98). These results provided the first example of an experiment where both the specific and non-specific Hg^{II} binding affinities could be derived from a single titration.

Table 1. Equilibrium binding affinity (K_d) of Hg^{II} binding to ^{DMA}T-containing duplex DNAs.^a

Sequence	K_d (nM) non-specific	K_d (nM) T-T-specific
X13 ^{DMA} T-A	1970 \pm 80	<i>n.o.</i> ^b
X13 ^{DMA} T-T	<i>n.o.</i> ^b	77 \pm 4
X13 ^{DMA} T-A, X16 T-T	1960 \pm 50	<i>n.o.</i> ^b
X14 ^{DMA} T-A, X16 T-T	2200 \pm 90	34 \pm 12
X15 ^{DMA} T-A, X16 T-T	<i>n.o.</i> ^b	57 \pm 7

^a Reported values = mean \pm standard deviation from three independent measurements. Samples contained 25 nM of DNA in an aqueous buffer containing 200 mM of Na₂HPO₄, 100 mM citric acid and 100 mM NaNO₃ (pH = 7.35). K_d values were calculated by fitting quenching data to a monoexponential curve (eq. 1 – 4, SI), except for “X14^{DMA}T-A, X16 T-T” which was fit to a biphasic curve (eq. 5, SI). In all cases, R^2 values were \geq 0.94. For duplex DNA sequences see Table S1, SI. ^b “*n.o.*” = not observed.

Kinetic analysis of T-Hg^{II}-T binding. Time-dependent changes in fluorescence were used to measure Hg^{II} association rates by duplexes containing a single ^{DMA}T-T mismatch at position X13 or X15, or an unmodified T-T mismatch adjacent to a ^{DMA}T-A base pair in “X15^{DMA}T-A, X16 T-T”. Control experiments with duplexes containing a ^{DMA}T-A base pair but no T-T mismatch exhibited an extremely rapid and small magnitude of fluorescence quenching (<10%) upon addition of Hg^{II} (Figures S6 – S7, SI). This non-specific component was excluded from our data analysis. Association rates and rate constants (k_{on}) were determined using pseudo-first-order approximations (eq. 6 – 9, SI) at three mercury concentrations. Similar k_{on} values were obtained for all three duplexes, ranging from $0.8 - 9.0 \times 10^4$ s⁻¹ (Table 2). These rate constants are about 10⁵-fold lower than those reported for outer-sphere binding of divalent ions to polynucleotides.²⁸ This is consistent with the fact that T-Hg^{II}-T binding requires N3-H deprotonation to give a stable complex. It was unclear how this multi-

step process might impact our kinetics analyses, but the excellent agreement between the K_d values determined by both kinetic and thermodynamic methods indicate a negligible effect (Tables 1 – 2).

To measure the rate constants of mercury dissociation (k_{off}) from duplexes containing ^{DMA}T-Hg^{II}-T or T-Hg^{II}-T, a large excess of an analogous, non-fluorescent duplex DNA containing a T-T mismatch was added as a passive Hg^{II} scavenger. The addition of 40 equiv. of unlabeled DNA was needed to obtain a concentration-independent, first order dissociation curve (Figure 4b). By fitting the data to a single-order decay process, k_{off} was calculated from the obtained half-lives ($t_{1/2}$) (eq. 11 – 12, SI). Similar k_{off} values were obtained for all three duplexes evaluated, ranging from $1.5 - 9.0 \times 10^{-4}$ s⁻¹ (Table 2), corresponding to $t_{1/2}$ values of 0.3 – 1.3 h.

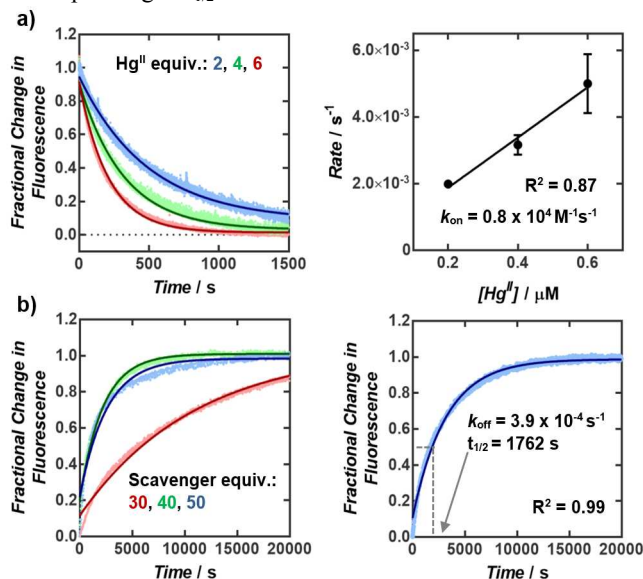


Figure 4. (a) Association of Hg^{II} to “X13^{DMA}T-T” according to fluorescence changes (λ_{ex} = 370 nm, λ_{em} = 500 nm). Rate constants of association (k_{on}) were determined from the slopes of reaction rate versus Hg^{II} concentration. (b) Dissociation of Hg^{II} from “X13^{DMA}T-T” upon the addition of unlabeled, T-T-containing duplex DNA. ^{DMA}T-Hg^{II}-T and T-Hg^{II}-T base pairs were formed by pre-incubation of the DNA with 2 equiv. of Hg(ClO₄)₂ for 3 h. All samples contained 0.1 μ M (k_{on}) or 4 μ M (k_{off}) of DNA in aqueous buffer (200 mM of Na₂HPO₄, 100 mM of citric acid and 100 mM NaNO₃ (pH = 7.35)). For raw data see Figures S8 – S10, SI.

Table 2. Rate constants of association (k_{on}), dissociation (k_{off}), and calculated equilibrium affinities (K_d) of Hg^{II} binding to ^{DMA}T-T or T-T in duplex DNA.^a

Sequence	k_{on} (M ⁻¹ s ⁻¹)	k_{off} (s ⁻¹)	K_d (nM) ^c
X13 ^{DMA} T-T	$0.8 \pm 0.2 \times 10^4$	$4.0 \pm 0.5 \times 10^{-4}$	50 ± 14
X15 ^{DMA} T-T ^b	$1.9 \pm 0.1 \times 10^4$	$1.5 \pm 0.2 \times 10^{-4}$	8.0 ± 1.1
X15 ^{DMA} T-A, X16 T-T	$9.0 \pm 2.0 \times 10^4$	$9.0 \pm 4.0 \times 10^{-4}$	10 ± 5.0

^a Reported values = mean \pm standard deviation from three independent measurements. Dissociation rate constants were determined by addition of 50 equiv. of unlabeled DNA containing a T-T mismatch. All samples were prepared in aqueous buffer (200 mM of Na₂HPO₄, 100 mM of citric acid and 100 mM NaNO₃ (pH = 7.35)). ^b Similar rates constants of association and dissociation were also observed for duplex X15^{DMA}T-T when measurements were conducted in a buffer containing 10 mM cacodylic acid and 100 mM NaClO₄ (pH = 6.8). ^c Equilibrium dissociation constants (K_d) calculated as $K_d = k_{off} / k_{on}$.

T-Hg^{II}-T base pairs inhibit DNA-DNA strand-displacement. Most biochemical processes take place on time scales ranging from microseconds to seconds. The exceptionally high kinetic stabilities of T-Hg^{II}-T base pairs could therefore pose significant barriers to DNA metabolism. To evaluate this possibility, DNA-DNA strand-displacement was selected as a model system for T-loop and R-loop dynamics.²⁹ Duplexes with a short single-stranded overhang (green, Figure 5 and Table S2, SI) were prepared containing either ^{DMA}T-Hg^{II}-T or a ^{DMA}T-A base pair located 3 to 4 base pairs away from an unmodified T-Hg^{II}-T. Strand-displacement of the ^{DMA}T-containing strand was initiated by adding a large excess of an unlabeled invading strand “I” to give a longer, thermodynamically more stable duplex as the product. Changes in ^{DMA}T fluorescence were used to track strand-displacement reactions in real time (Figures S11 – S16, SI). Second-order rate constants were calculated under pseudo-first order conditions (eq. 14, SI) by adding 4, 6, 8, or 10 equiv. of the invading strand. In the absence of Hg^{II}, the rate constants for all duplexes ranged from 29 – 247 M⁻¹s⁻¹, corresponding to experimental half-lives of 1.5 – 33 min. In contrast, 100 to 2000-fold lower rate constants ($k = 0.05 - 0.47$ M⁻¹s⁻¹) were measured for the same duplexes containing a single ^{DMA}T-Hg^{II}-T or T-Hg^{II}-T, corresponding to experimental half-lives of 10 – 77 hours. Duplexes lacking a T-T mismatch exhibited the same displacement rates in both the presence and absence of Hg^{II} (Table 3), indicating that non-specific Hg^{II}-DNA binding had little or no impact on strand displacement kinetics. Taken together, these results demonstrate that T-Hg^{II}-T base pairs impose a large and specific kinetic barrier to passive DNA-DNA strand-displacement reactions.

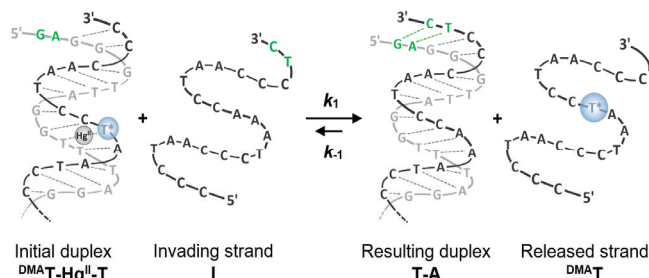


Figure 5. Schematic representation of a strand-displacement reaction, where $T^* = {}^{\text{DMA}}\text{T}$.

Table 3. Second-order rate constants k (M⁻¹s⁻¹) of strand-displacement in the absence or presence of Hg^{II}.^a

Initial Duplex	k (M ⁻¹ s ⁻¹), no Hg ^{II}	k (M ⁻¹ s ⁻¹), + Hg ^{II}
X13 ^{DMA} T-T	97 ± 12	0.05 ± 0.01
X13 ^{DMA} T-A, X10 T-T	55 ± 15	0.47 ± 0.03
X13 ^{DMA} T-A, X16 T-T	247 ± 16	0.21 ± 0.06
X13 ^{DMA} T-A	29 ± 3.0	22 ± 3.0 ^b

^a Reported values = mean ± standard deviation of three independent rate constant measurements. All samples contained 4 μM of duplex DNA in aqueous buffer (200 mM of Na₂HPO₄, 100 mM of citric acid and 100 mM NaNO₃ (pH = 7.35)). ^{DMA}T-Hg^{II}-T and T-Hg^{II}-T base pairs were generated by incubating the DNA with 2 equiv. of Hg(ClO₄)₂ for 3 h. Similar results were obtained when the probe was positioned at **X14** (Figure S16, Table S3, SI). ^b This rate constant was estimated from a single “I” concentration, see Figure S13, SI.

T-Hg^{II}-T base pairs inhibit DNA polymerases. To evaluate the potential impact of T-Hg^{II}-T base pairs on energy-dependent strand-displacement reactions, we investigated enzymatic DNA synthesis by two different DNA polymerases differing only in their exonuclease (*exo*) activities: DNA Pol I from *E. coli* (5' to 3' *exo*+), and the derived “Klenow Fragment” (5' to 3' *exo*-). Primer extension assays were conducted using DNA duplexes containing either a T-T or T-A base pair at position #1 (ODN1) or position #7 (ODN2) downstream of a nicked site (arrow, Figure 6a). DNA synthesis therefore requires displacement or degradation of the non-template “displaced strand” DNA. The primer-template constructs were incubated with variable concentrations of Hg^{II} (0 – 20 μM) for three hours, followed by addition of nucleotide triphosphates and a DNA polymerase. Aliquots from each reaction were removed as a function of time, quenched with EDTA and analyzed by denaturing polyacrylamide gel electrophoresis (PAGE, Figure 6b, Figures S17 – S24, SI).

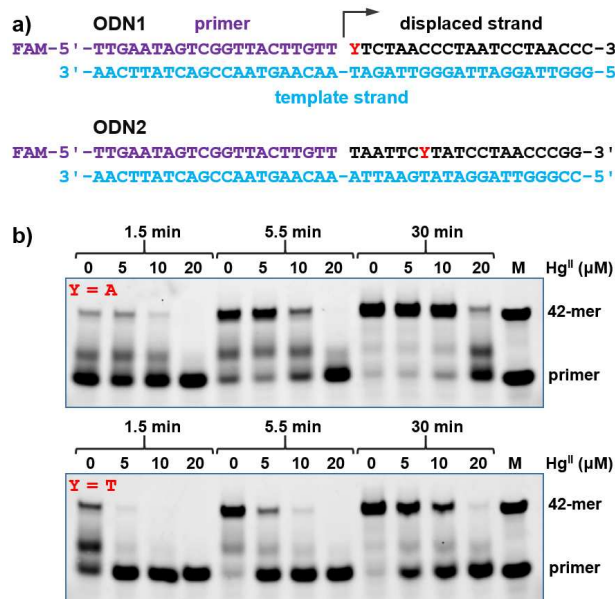


Figure 6. (a) Duplex DNAs “ODN1” and “ODN2” containing a Watson-Crick base pair (Y=A), or T-T mismatch (Y=T) where “FAM” = fluorescein. (b) PAGE analysis of ODN1 primer extension by the Klenow Fragment at various Hg^{II} concentrations and time points. “M” = marker for primer and full-length sequence.

Hg^{II} caused both specific and non-specific inhibition of primer extension as revealed by duplexes containing T-T versus T-A, respectively. DNA synthesis by the Klenow Fragment (*exo*-) requires DNA strand displacement of the non-template strand in a 5' to 3' direction. As such, a 2.7-fold higher rate of primer extension was observed for ODN1 containing T-T versus T-A in the absence of Hg^{II} (Table 4). Upon adding 5 – 10 μM of Hg^{II}, a 7 to 13-fold decrease in k_{obs} was observed for ODN1 containing T-T, whereas little or no change was observed for the same duplex containing a T-A base pair (Klenow, Table 4). Given the relatively slow k_{on} rates for Hg^{II} binding to T-T (Figure 4a), the inhibition of Klenow by T-Hg^{II}-T must be the result of a slow off rate of Hg^{II} from the duplex-enzyme complex. Similar inhibitory effects of a smaller magnitude were observed for ODN2 that exhibited a

pronounced stalling and termination of DNA synthesis at the T-Hg^{II}-T site (Figure S21, Table S4, SI).

In contrast to the Klenow Fragment, DNA synthesis by *E. coli* DNA Pol I involves the enzymatic degradation of the non-template DNA strand in a 5' to 3' direction. As such, in the absence of Hg^{II}, the same rates of primer extension were observed for ODN1 containing T-A versus T-T (Table 4). Interestingly, upon adding 5 – 10 μ M of Hg^{II}, a 2-fold decrease in k_{obs} was observed for ODN1 containing T-T, whereas a roughly 2-fold increase in k_{obs} was observed for ODN1 containing T-A (Pol I, Table 4). These results demonstrate that T-Hg^{II}-T sites impose a specific barrier to DNA synthesis that cannot be entirely overcome by exonuclease activity. Interestingly, the Hg^{II} concentrations needed for DNA polymerase inhibition *in vitro* (IC₅₀ = 6.3 μ M – 17.5 μ M, Figure S18 and S22, SI) were in the same concentration range as those reported to perturb DNA synthesis in living cells.^{5b}

Table 4. Observed rates (k_{obs}) of ODN 1 primer extension by Klenow Fragment (*exo-*) or *E. coli* DNA Pol I (*exo+*).^a

Hg ^{II} (μ M)	“Y”	Klenow (<i>exo-</i>) k_{obs} (min ⁻¹)	k_{obs} rel (<i>exo-</i>)	Pol I (<i>exo+</i>) k_{obs} (min ⁻¹)	k_{obs} rel (<i>exo+</i>)
0	A	0.18 ± 0.05	1.0	0.20 ± 0.02	1.0
	T	0.48 ± 0.12	1.0	0.21 ± 0.04	1.0
5	A	0.23 ± 0.07	1.3	0.23 ± 0.06	1.2
	T	0.07 ± 0.01	0.15	0.16 ± 0.06	0.76
10	A	0.14 ± 0.05	0.8	0.35 ± 0.16	1.8
	T	0.038 ± 0.002	0.08	0.11 ± 0.05	0.52
20	A	0.044 ± 0.005	0.24	0.17 ± 0.10	0.85
	T	0.04 ± 0.02	0.08	0.05 ± 0.01	0.24

^a For experimental details see Materials and Methods. The relative rates “ k_{obs} rel” = k_{obs} (X μ M Hg) / k_{obs} (0 μ M Hg), where X = 5, 10 or 20.

DISCUSSION AND CONCLUSIONS

The formation and properties of “all-natural” metallo base pairs such as T-Hg^{II}-T and C-Ag^I-C have broad implications in materials and biological sciences.³⁰ Previous studies have demonstrated that T-Hg^{II}-T base pairs exhibit similar thermal stabilities and structural features as T-A base pairs in duplex DNA.¹⁰⁻¹² The perception of analogous behavior of T-Hg^{II}-T and T-A was further enhanced by studies showing that T-Hg^{II}-T could serve as a substitute for T-A in primer hybridization,¹³ and by the enzymatic misincorporation of dTTP across from thymidine to give T-Hg^{II}-T base pairs in the new duplex.¹⁴ This activity could provide a pathway for the formation of T-Hg^{II}-T base pairs in genomic DNA that explains some of the point mutations known to occur in cells treated with Hg^{II}.³

The kinetic parameters of mercury binding reactions are expected to be highly relevant *in vivo*, where high concentrations of protein thiols and glutathione (20 – 50 mM total) would be expected to easily out-compete DNA for Hg^{II} binding.³¹ Amazingly, the addition of micromolar concentrations of Hg^{II} (5 μ M) to living cells resulted in the formation of high-stability DNA-Hg^{II} adducts at a frequency of 0.3% of all base pairs.⁷ This is approximately the same concentration of Hg^{II} that was needed to inhibit DNA polymerase inhibition *in vitro*

(Table 4) and to perturb DNA synthesis in living cells.^{5b} Given the vast excess of intracellular thiols and irreversible binding of S-Hg^{II}-S, thermodynamic parameters alone cannot explain these observations.

Here we report the first kinetic analysis of Hg^{II} binding to T-T sites in duplex DNA. Contrary to the common perception of analogous structural and functional properties of T-Hg^{II}-T and T-A,¹⁰⁻¹⁴ our results demonstrate that T-Hg^{II}-T base pairs are kinetically distinct from T-A base pairs. The slow on-rates and extremely slow off-rates of Hg^{II} from T-T are consistent with the formation and breakage of partially covalent bonds. Agreements between our kinetic and thermodynamic analyses were remarkably good, both giving affinities in the range of K_d = 8 – 77 nM. In contrast, duplexes lacking a T-T mismatch exhibited local, “non-specific” Hg^{II} binding affinities of K_d = 0.20 – 2.0 μ M, depending on the coordination strength of the buffer. The non-specific components of Hg^{II} association reactions were extremely rapid (Figure S7, SI), consistent with outer-sphere binding of divalent ions that are near the diffusion limits.²⁸ Given these observations together, we propose a model for Hg^{II} exposure of living cells, where long-range electrostatic interactions facilitate rapid, non-specific association of Hg^{II} to the N1 or N7 positions of purines⁹ that offer some temporary protection from cellular thiols. Cells in S-phase then incorporate Hg^{II} ions into DNA as T-Hg^{II}-T mismatches that exhibit high kinetic stabilities and therefore disrupt a wide variety of processes. Here we demonstrate that T-Hg^{II}-T base pairs are inhibitors of DNA polymerases that would normally displace or degrade the non-template DNA strand during DNA synthesis. These activities are required for DNA repair and the completion of DNA lagging strand synthesis.³² Indeed, Hg^{II} is known to cause the inhibition of both DNA synthesis and repair in living cells.^{5,6} The ability of Hg^{II} to inhibit DNA polymerases *in vitro* also reveals a potential mechanism for its reported ability to cause DNA strand breaks *in vivo*,^{4,5} where molecules that generate DNA-DNA inter-strand crosslinks can cause DNA strand breaks due to cellular metabolism.³³ The premature termination of DNA synthesis is one such mechanism by which this can occur (Figure S21). It is possible that other dynamic processes such as transcription and DNA repair are also directly inhibited by the high kinetic stabilities of T-Hg^{II}-T base pairs.

MATERIALS AND METHODS

DNA synthesis. DNA oligonucleotides containing a single DNA⁺T at variable positions “X” were synthesized using phosphoramidite chemistry, purified and characterized as previously reported.²⁶ Oligonucleotide stock solutions were prepared in pure water. Double-stranded oligonucleotides were formed by mixing equal amounts of the complementary oligonucleotides in the indicated buffer and heating to 95 °C for 5 min, and slowly cooling to room temperature over 4 h. DNA⁺T-Hg^{II}-T and T-Hg^{II}-T base pairs were formed by incubating 2 equiv. of Hg(ClO₄)₂ with the DNA solutions for 3 h prior to use.

Thermodynamic measurements. Equilibrium dissociation constants (K_d) were measured in three independent trials using a Horiba FluoroLog spectrofluorometer equipped with a speed stirrer and a temperature controller. Pre-folded duplex DNA (4 μ M) in aqueous buffer (200 mM Na₂HPO₄, 100 mM citric acid, 100 mM NaNO₃ (pH = 7.35), or alternatively,

10 mM sodium cacodylate-cacodylic acid, 100 mM Na(ClO₄)₂ (pH = 6.8) was diluted to 25 nM in a 1.5 mL cuvette. Aliquots of Hg(ClO₄)₂ were added while stirring at 25°C and the fluorescent intensity was measured after a 1 h incubation.

Kinetic measurements. Association rate constants (k_{on}) were measured in three independent trials using a Horiba FluoroLog spectrofluorophotometer equipped with a speed stirrer and a temperature controller. Pre-folded duplex DNA (4 μ M) in aqueous buffer (200 mM Na₂HPO₄, 100 mM citric acid and 100 mM NaNO₃) was diluted to a final concentration of 0.1 μ M in a 1.5 ml cuvette. Hg(ClO₄)₂ (2, 4, and 6 equiv.) was added under stirring and the fluorescent intensity was measured as a function of time (λ_{ex} = 370 nm, λ_{em} = 500 nm) at 25°C.

Dissociation rate constant (k_{off}) measurements were measured in three independent trials using a Molecular Devices Spectra spectrofluorophotometer with a temperature controller in 384-wellplates. Pre-folded duplex DNA (4 μ M) in aqueous buffer (200 mM Na₂HPO₄, 100 mM citric acid and 100 mM NaNO₃, pH = 7.35) was incubated with 2 equiv. of Hg(ClO₄)₂ for 3 h at rt. Then, 50 equiv. of an unlabeled duplex DNA of the same sequence containing a T-T mismatch was added as a passive Hg^{II} scavenger, the mixture was rapidly mixed and then overlaid with paraffin oil. The increase of fluorescent intensity was measured as a function of time (λ_{ex} = 370 nm, λ_{em} = 500 nm) at 25°C. Similar results were obtained when using a scavenger duplex DNA having a different sequence, suggesting the absence of any strand-displacement activity during the k_{off} measurements.

Strand-displacement measurements. Strand-displacement reactions were carried out in three independent trials as previously described.²⁹ To pre-folded ^{DMA}T-modified duplexes DNA (4 μ M) containing a 5'-overhang, an excess of invading strand was added (Table S2). The reaction was rapidly mixed, overlaid with paraffin oil, and changes in fluorescent intensity were measured as a function of time (λ_{ex} = 370 nm, λ_{em} = 500 nm) at 25 °C.

Primer extension reactions. dNTP's were purchased as 100 mM solutions from *New England BioLabs Inc.* Klenow Fragment (3' → 5' *exo*-) and DNA Pol I (*E. coli*) were purchased from *New England BioLabs Inc.* Prior to use, the buffers were exchanged by ultrafiltration at 12500 x g utilizing an Amicon Ultra-0.5 centrifugal filter. The buffer solution containing Klenow Fragment (*exo*-) was exchanged with 25 mM Tris-HCl, 1 mM 3,3',3"-phosphanetriyltris (benzenesulfonic acid) trisodium salt (TPPTS), 0.1 mM EDTA and 50 % glycerol at pH = 7.40. The buffer solution containing DNA Pol I (*E. coli*) was exchanged with 25 mM Tris-HCl, 0.11 mM TPPTS, 11 μ M EDTA and 50 % glycerol at pH = 7.40.

Template strands were annealed with complementary sequences and a 5' FAM-labeled primer at 10 μ M each. After heating and slow cooling to rt, Hg(ClO₄)₂ was added (0 – 200 equiv.) and incubated for 3 h at rt. The mixture was diluted to a final concentration of 100 nM. dNTP's were then added and the reaction was started by the addition of DNA polymerase. The total reaction volume was 70 μ L, and the final concentrations of each component was 100 nM template strand, 100 nM primer, 100 nM complementary strand, 2 μ M dNTPs, and 50 nM Klenow Fragment (*exo*-) or 0.05 nM DNA Pol I (*E. coli*). The reaction mixture was incubated at 25 °C or 37 °C, for Klenow Fragment and DNA Pol I, respectively. Final buffer

conditions were 50 mM NaCl, 10 mM MgCl₂ and 10 mM Tris-HCl, 8 μ M TPPTS (pH = 7.90). Aliquots of each reaction (10 μ L) were removed at the given time point and quenched by the addition of loading solution (10 μ L, 8 M urea, 30 mM EDTA, 50 % sucrose) and heating at 90 °C for 10 min. The reaction mixtures were then placed on ice and a DTT solution (1 μ L, 100 mM) was added to bind Hg^{II} thereby preventing aggregation of the DNA.¹⁴ The reactions components were separated by gel electrophoresis on a 13 % polyacrylamide gel (1 x TBE) under denaturing conditions (8 M urea). Gels were scanned on *Typhoon FLA 9500* (λ_{ex} = 473 nm, λ_{em} = 520 nm) and analyzed using *ImageQuantTL*.

ASSOCIATED CONTENT

Supporting Information. Equations, Figures S1 – S24, Tables S1 – S5, and additional fluorescence spectra. This material is available free of charge via the Internet at <http://pubs.acs.org>.

AUTHOR INFORMATION

Corresponding Author

* Prof. Dr. Nathan W. Luedtke, nathan.luedtke@chem.uzh.ch

ACKNOWLEDGMENT

We gratefully acknowledge the Swiss National Science Foundation for generous financial support (grant #165949) and the University of Zürich. We thank Franziska Zosel, Prof. Dr. Ben Schuler and his group for their technical assistance.

REFERENCES

- (1) Park, J.-D.; Zheng, W. *J. Prev. Med. Public Heal.* **2012**, *45*, 344.
- (2) Monteiro, D. A.; Rantin, F. T.; Kalinin, A. L.; *Ecotoxicology*, **2010**, *19*, 105.
- (3) a) Schurz, F.; Sabater-Vilar, M.; Fink-Gremmels, J.; *Mutagen.* **2000**, *15*, 525; b) Codina, J. C.; Pérez-Torrente, C.; Pérez-García, A.; Cazorla, F. M.; deVicente, A.; *Arch. Environ. Contam. Toxicol.* **1995**, *29*, 260. c) Ariza M. E.; Williams, M. V. *J. Biochem. Mol. Toxicol.* **1999**, *13*, 107.
- (4) Cantoni, O.; Evans, R. M.; Costa, M. *Biochem. Biophys. Res. Commun.* **1982**, *108*, 614.
- (5) Williams, M. V.; Winters, T.; Waddell, K. S. *Mol. Pharmacol.* **1987**, *31*, 200.
- (6) Christie, N. T.; Cantoni, O.; Sugiyama, M.; Cattabeni, F.; Costa, M. *Mol. Pharmacol.* **1986**, *29*, 173.
- (7) Cantoni, O.; Christie, N. T.; Swann, A.; Drath, D. B.; Costa, M. *Mol. Pharmacol.* **1984**, *26*, 360.
- (8) a) Clever, G. H.; Kaul, C.; Carell, T. *Angew. Chem. Int. Ed.* **2007**, *46*, 6226; b) Megger, D. A.; Megger, N.; Müller J. in *Metal Ions in Life Sciences*, Vol. 10 (Eds.: Sigel, A.; Sigel, H.; Sigel R. K. O.), Springer, Dordrecht, **2012**, 295-317; c) Takezawa, Y.; Shionoya, M. *Acc. Chem. Res.* **2012**, *45*, 2066; d) Clever, G. H.; Shionoya M. in *Metal Ions in Life Sciences*, Vol. 10 (Eds.: Sigel, A.; Sigel, H.; Sigel R. K. O.), Springer, Dordrecht, **2012**, 269-294.
- (9) a) Simpson, R. B. *J. Am. Chem. Soc.* **1964**, *86*, 2059; b) Buchanan, G. W.; Stothers, J. B. *Can. J. Chem.* **1982**, *60*, 787; c) Polak, M.; Plavec, J. *Eur. J. Inorg. Chem.* **1999**, 547; d) Eichhorn, G. L.; Clark, P. *J. Am. Chem. Soc.* **1963**, *85*, 4020.
- (10) Miyake, Y.; Togashi, H.; Tashiro, M.; Yamaguchi, H.; Oda, S.; Kudo, M.; Tanaka, Y.; Kondo, Y.; Sawa, R.; Fujimoto, T.; Machinami, T.; Ono, A. *J. Am. Chem. Soc.* **2006**, *128*, 2172.
- (11) Tanaka, Y.; Oda, S.; Yamaguchi, H.; Kondo, Y.; Kojima, C.; Ono, A. *J. Am. Chem. Soc.* **2007**, *129*, 244.

- (12) Kondo, J.; Yamada, T.; Hirose, C.; Okamoto, I.; Tanaka, Y.; Ono, A. *Angew. Chem. Int. Ed.* **2014**, *53*, 2385.
- (13) Park, K. S.; Jung, C.; Park, H. G. *Angew. Chem. Int. Ed.* **2010**, *49*, 9757.
- (14) Urata, H.; Yamaguchi, E.; Funai, T.; Matsumura, Y.; Wada, S.-I. *Angew. Chem. Int. Ed.* **2010**, *49*, 6516.
- (15) a) Liu, J.; Lu, Y. *Angew. Chem. Int. Ed.* **2007**, *46*, 7587; b) Li, D.; Wieckowska, A.; Willner, I. *Angew. Chem. Int. Ed.* **2008**, *47*, 3927; c) Liu, C.-W.; Lin, Y.-W.; Huang, C.-C.; Chang, H.-T. *Biosens. Bioelectron.* **2009**, *24*, 2541; d) Mor-Piperberg, G.; Tel-Vered, R.; Elbaz, J.; Willner, I. *J. Am. Chem. Soc.* **2010**, *132*, 6878; e) Wang, Z.-G.; Elbaz, J.; Willner, I. *Nano Lett.* **2011**, *11*, 304; f) Wen, S.; Zeng, T.; Liu, L.; Zhao, K.; Zhao, Y.; Liu, X.; Wu, H.-C. *J. Am. Chem. Soc.* **2011**, *133*, 18312; g) Thomas, J. M.; Yu, H.-Z.; Sen, D. *J. Am. Chem. Soc.* **2012**, *134*, 13738; h) Xiao, S. J.; Hu, P. P.; Xiao, G. F.; Wang, Y.; Liu, Y.; Huang, C. Z. *J. Phys. Chem. B*, **2012**, *116*, 9565; i) Kang, I.; Wang, Y.; Reagan, C.; Fu, Y.; Wang, M. X.; Gu, L.-Q. *Sci. Rep.* **2013**, *3*, 2381; j) Scharf, P.; Müller, J. *ChemPlusChem*, **2013**, *78*, 20.
- (16) a) Gruenwedel, D. W.; Cruikshank, M. K.; Smith, G. M. *J. Inorg. Biochem.* **1993**, *52*, 251; b) Gruenwedel, D. W. *Biophys. Chem.* **1994**, *52*, 115; c) Tanaka, Y.; Yamaguchi, H.; Oda, S.; Kondo, Y.; Nomura, M.; Kojima, C.; Ono, A. *Nucleosides, Nucleotides and Nucleic Acids*, **2006**, *25*, 613.
- (17) a) Chrisman, R. W.; Mansy, S.; Peresie, H. J.; Ranade, A.; Berg, T. A.; Tobias, R. S. *Bioinorg. Chem.* **1977**, *7*, 245; b) Uchiyama, T.; Miura, T.; Takeuchi, H.; Dairaku, T.; Komuro, T.; Kawamura, T.; Kondo, Y.; Benda, L.; Sychrovský, V.; Bouř, P.; Okamoto, I.; Ono, A.; and Tanaka, Y. *Nucleic Acids Res.* **2012**, *40*, 5766.
- (18) a) Gruenwedel, D. W. *J. Inorg. Biochem.* **1994**, *56*, 201; b) Kuklenyik, Z.; Marzilli, L. G. *Inorg. Chem.* **1996**, *35*, 5654.
- (19) a) Tanaka, Y.; Ono, A. *Dalton Trans.* **2008**, 4965; b) Dairaku, T.; Furuita, K.; Sato, H.; Šebera, J.; Yamanaka, D.; Otaki, H.; Kikkawa, S.; Kondo, Y.; Katahira, R.; Bickelhaupt, F. M.; Guerra, C. F.; Ono, A.; Sychrovský, V.; Kojima, C.; Tanaka, Y. *Chem. Commun.* **2015**, *51*, 8488.
- (20) a) Torigoe, H.; Ono, A.; Kozasa, T. *Chem. Eur. J.* **2010**, *16*, 13218; b) Torigoe, H.; Miyakawa, Y.; Ono, A.; Kozasa, T. *Thermochim. Acta*, **2012**, *532*, 28. c)
- (21) a) Ono, A.; Togashi, H. *Angew. Chem. Int. Ed.* **2004**, *43*, 4300; b) Liu, C.-W.; Hsieh, Y.-T.; Huang, C.-C.; Lin, Z.-H.; Chang, H.-T. *Chem. Commun.* **2008**, 2242; c) Wang, J.; Liu, B. *Chem. Commun.* **2008**, 4759; d) Xue, X.; Wang, F.; Liu, X. *J. Am. Chem. Soc.* **2008**, *130*, 3244; e) Yang, R.; Jin, J.; Long, L.; Wang, Y.; Wang, H.; Tan, W. *Chem. Commun.* **2009**, 322.
- (22) For review articles see: a) Okamoto, A.; Saito, Y.; Saito, I. *J. Photochem. Photobiol. Photochem. Rev.* **2005**, *6*, 108; b) Sinkeldam, R. W.; Greco, N. J.; Tor, Y. *Chem. Rev.* **2010**, *110*, 2579; c) Wilhelmsson, L. M.; *Q. Rev. Biophys.* **2010**, *43*, 159; d) Tanpure, A. A.; Pawar, M. G.; Srivatsan, S. G. *Isr. J. Chem.*, **2013**, *53*, 366; e) Jones, A. C.; Neely, R. K. *Q. Rev. Biophys.*, **2015**, *48*, 244. f) Matarazzo, A.; Hudson, R. H. E. *Tetrahedron*, **2015**, *71*, 1627.
- (23) For selected examples see: a) Okamoto, A.; Tanaka, K.; Saito, I. *J. Am. Chem. Soc.* **2003**, *125*, 4972; b) Sun, K. M.; McLaughlin, C. K.; Lantero, D. R.; Manderville, R. A. *J. Am. Chem. Soc.* **2007**, *129*, 1894; c) Jiang, D.; Seela, F.; *J. Am. Chem. Soc.* **2010**, *132*, 4016; d) Dumas, A.; Luedtke, N. W. *Nucleic Acids Res.* **2011**, *39*, 6825; e) Dumas, A.; Luedtke, N. W. *ChemBioChem*, **2011**, *12*, 2044; f) Riedl, J.; Pohl, R.; Rulisek, L.; Hocek, M. *J. Org. Chem.* **2012**, *77*, 1026; g) Segal, M.; Fischer, B. *Org. Biomol. Chem.* **2012**, *10*, 1571; h) Saito, Y.; Suzuki, A.; Okada, Y.; Yamasaka, Y.; Nemoto, N.; Saito, I. *Chem. Commun.* **2013**, *49*, 5684; i) Seio, K.; Kanamori, T.; Tokugawa, M.; Ohzeki, H.; Masaki, Y.; Tsunoda, H.; Ohkubo, A.; Sekine, M. *Bioorg. Med. Chem.* **2013**, *21*, 3197; j) Weinberger, M.; Berndt, F.; Mahrwald, R.; Ernsting, N. P.; Wagenknecht, H. A. *J. Org. Chem.*, **2013**, *78*, 2589; k) Rodgers, B. J.; Elsharif, N. A.; Vashisht, N.; Mingus, M. M.; Mulvahill, M. A.; Stengel, G.; Kuchta, R. D.; Purse, B. W. *Chem. Eur. J.* **2014**, *20*, 2010; l) Suchy, M.; Hudson, R. H. E. *J. Org. Chem.* **2014**, *79*, 3336; m) McCoy, L. S.; Shin, D.; Tor, Y. *J. Am. Chem. Soc.* **2014**, *136*, 15176; n) Kanamori, T.; Ohzeki, H.; Masaki, Y.; Ohkubo, A.; Takahashi, M.; Tsudo, K.; Ito, T.; Shirouzu, M.; Kuwasako, K.; Muto, Y.; Sekine, M.; Seio, K. *ChemBioChem*, **2015**, *16*, 167; o) Larsen, A. F.; Dumat, B.; Wranne, M. S.; Lawson, C. P.; Preus, S.; Bood, M.; Gradén, H.; Wilhelmsson, L. M.; Grötl, M. *Nat. Publ. Gr.* **2015**, *1*; p) Sholokh, M.; Sharma, R.; Shin, D.; Das, R.; Zaporozhets, O. A.; Tor, Y.; Mély, Y. *J. Am. Chem. Soc.* **2015**, *137*, 3185; q) Mata, G.; Luedtke, N. W. *J. Am. Chem. Soc.* **2015**, *137*, 699; r) Mizrahi, R. A.; Shin, D.; Sinkeldam, R. W.; Phelps, K. J.; Fin, A.; Tantillo, D. J.; Tor, Y.; Beal, P. A. *Angew. Chem. Int. Ed.* **2015**, *54*, 8713; s) Tanpure, A. A.; Srivatsan, S. G. *Nucleic Acids Res.* **2015**, *43*, e149.
- (24) a) Fedoriw, A. M.; Liu, H.; Anderson, V. E.; deHaseth, P. L. *Biochemistry*, **1998**, *37*, 11971; b) Arzumanov, A.; Godde, F.; Moreau, S.; Toulme, J.; Weeds, A.; Gait, M. J. *Helv. Chim. Acta*, **2000**, *83*, 1424; c) Bradrick, T. D.; Marino, J. P. *RNA*, **2004**, *10*, 1459; d) Gilbert, S. D.; Stoddard, C. D.; Wise, S. J.; Batey, R. T. *J. Mol. Biol.* **2006**, *359*, 754; e) Kimura, T.; Kawai, K.; Fujitsuka, M.; Majima, T. *Tetrahedron*, **2007**, *63*, 3585; f) Parsons, J.; Hermann, T. *Tetrahedron*, **2007**, *63*, 3548; g) Lang, K.; Rieder, R.; Micura, R. *Nucleic Acids Res.* **2007**, *35*, 5370; h) Barbieri, C. M.; Kaul, M.; Pilch, D. S. *Tetrahedron*, **2007**, *63*, 3567; i) Xie, Y.; Dix, A. V.; Tor, Y. *J. Am. Chem. Soc.* **2009**, *131*, 17605; j) Velmurugu, Y.; Chen, X.; Sevilla, P. S.; Min, J.-H.; Ansari, A. *Proc. Natl. Acad. Sci.* **2016**, *113*, E2296.
- (25) a) Kim, S. J.; Kool, E. T. *J. Am. Chem. Soc.* **2006**, *128*, 6164; b) Dumas, A.; Luedtke, N. W. *Chem. Eur. J.* **2012**, *18*, 245; c) Omumi, A.; McLaughlin, C. K.; Ben-Israel, D.; Manderville, R. A. *J. Phys. Chem. B*, **2012**, *116*, 6158; d) Jana, S. K.; Guo, X.; Mei, H.; Seela, F. *Chem. Commun.* **2015**, *51*, 17301.
- (26) Mata, G.; Schmidt, O. P.; Luedtke, N. W. *Chem. Commun.* **2016**, *52*, 4718.
- (27) Martell, A. E.; Smith, R. M. *Critical Stability Constants, Vol. 4*, Plenum Press, New York, **1979**, 394.
- (28) a) Pörschke, D. *Biophys. Chem.* **1976**, *4*, 383; b) Granot, J.; Feigon, J.; Kearns, D. R. *Biopolymers*, **1982**, *21*, 181.
- (29) a) Yurke, B.; Turberfield, A. J.; Mills, A. P.; Simmel, F. C.; Neumann, J. L. *Nature*, **2000**, *406*, 605; b) Turberfield, A. J.; Mitchell, J. C.; Yurke, B.; Mills, A. P.; Blakey, M. I.; Simmel, F. C. *Phys. Rev. Lett.* **2003**, *90*, 118102; c) Zhang, D. Y.; Winfree, E. *J. Am. Chem. Soc.* **2009**, *131*, 17303; d) Zhang, D. Y.; Seelig, G.; *Nat. Chem.* **2011**, *3*, 103; e) Genot, A. J.; Zhang, D. Y.; Turberfield, A. J.; *J. Am. Chem. Soc.* **2011**, *133*, 2177; f) Tang, W.; Wang, H.; Wang, D.; Zhao, Y.; Li, N.; Liu, F. *J. Am. Chem. Soc.* **2013**, *135*, 13628.
- (30) Tanaka, Y.; Kondo, J.; Sychrovský, V.; Šebera, J.; Dairaku, T.; Saneyoshi, H.; Urata, H.; Torigoe, H.; Ono, A. *Chem. Commun.* **2015**, *51*, 17343.
- (31) Prakash, M.; Shetty, M.S.; Tilak, P.; Anwar, N. *Online J Health Allied Scs.* **2009**, *8*, 1.
- (32) a) Dianov, G. L.; Prasad, R.; Wilson, S. H.; Bohr, V. A. *J. Biol. Chem.* **1999**, *274*, 13741. b) Maga, G.; Villani, G.; Tillement, V.; Stucki, M.; Locatelli, G. A.; Frouin, I.; Spadari, S.; Hübscher, U. *Proc. Natl. Acad. Sci. U.S.A.*, **2001**, *98*, 14298.
- (33) Frankenberg-Schwager, M.; Kirchermeier, D.; Greif, G.; Baer, K.; Becker, M.; Frankenberg, D. *Toxicology*, **2005**, *212*, 175.

For Table of Contents Only

